

# Optical and Electrical Crosstalk in *PIN* Photodiode Array for Medical Imaging Applications

Ilja Goushcha, Bernd Tabbert and Alexander O. Goushcha, *Member of IEEE*

**Abstract** - Optical and electrical crosstalk are the parameters of photodetector arrays for medical imaging applications that often require special attention of the system developers and researchers. This paper studies crosstalk for the back-illuminated, thin *pin* photodiode arrays built on 75- $\mu\text{m}$  and 100- $\mu\text{m}$  thickness single silicon dies. The features of the arrays include high quantum efficiency, fast signal rise time, very small AC and DC electrical crosstalk ( $\sim 0.01\%$ ) within the spectral range 400 to 800 nm. The paper compares the noise performance and detectivity of back-illuminated photodiode arrays with isolating diffusion between pixels and conventional arrays with no isolation between pixels. Different sources of optical crosstalk in the scintillator-based X-ray imaging applications are discussed for two types of arrays. The noise characteristics and detectivity for the detector arrays with optical and electrical crosstalk were estimated to be 3-5 times better for the arrays with isolating diffusion than for the conventional photodiode arrays. A brief comparison with the front-illuminated arrays is also provided.

## I. INTRODUCTION

CURRENTLY, back-illuminated *pin* photodiode arrays occupy a key position in many array applications including two-dimensional and three-dimensional imaging. Advantages of back-illuminated arrays include, but are not limited to, small pixel and gap (dead spaces) size, no limitation on the number of pixels, high quantum efficiency across the whole spectral range, and fast response time. As a result, such arrays make high quality real time images possible.

While using back-illuminated photodiode arrays proved to be very efficient, there are still discussions about their advantages and drawbacks in comparison with the front-illuminated arrays. For example, the total crosstalk is known to be higher for the detector modules utilizing conventional back-illuminated (we will elaborate below the details of the corresponding structures), *pin* photodiode arrays than those using front-illuminated arrays [1].

A multi-slice x-ray detector is composed of a series of individual pixels in the *z*-axis (called slices) and a series of individual pixels in *x*-axis (called channels). Each individual pixel is composed of a scintillating crystal coupled to a silicon photodiode. The x-ray deposited in the scintillator is converted

to visible light. The efficiency of the x-ray to light conversion is mainly driven by the composition of the scintillating material and its activators. The pixels of the scintillator array are separated by a reflector (septa). The light quanta generated in the scintillator are then propagated through multiple reflections up to the surface of the photodiode where they are absorbed and converted to electron-hole charge.

In the scintillator-base x-ray imaging systems researchers separate usually four main different contributors to the crosstalk. One of them is a pure electrical crosstalk while the other three represent different kinds of an optical crosstalk [1-4]:

- 1) Pure electrical crosstalk arises due to a lateral drift/diffusion of non-equilibrium carriers created by light from the illuminated photodiode pixel to the neighbors. This source of the crosstalk is usually negligible if the photodiode array operates under the reverse bias since the electric field does not allow carriers to move perpendicular to the field gradient. However, for most of CT systems this source of the crosstalk is important since the photodiode arrays operate at zero bias. The value of this crosstalk component usually higher than  $\sim 0.1\%$  and may reach  $\sim 10\%$  of the signal strength dependently on the array structure.
- 2) Optical crosstalk that is created due to x-rays scattering from one scintillator pixel to the neighbors (which can be considered as x-ray crosstalk). This source may add up to several percent of the signal strength to the total crosstalk value.
- 3) Crosstalk that arises due to penetration of optical quanta created in the scintillator pixel through the reflective wall (septa) that separates two adjacent pixels in the scintillator array. These optical quanta ultimately reach the surface of the photodiode array where they can be absorbed within the area in between the active pixels, adding to the total optical crosstalk as much as up to a few percent of the signal strength.
- 4) Crosstalk due to leaking of optical radiation from the illuminated scintillator pixel via the layer of optical cement that separates the scintillator array and the surface of a photodiode array (a kind of a waveguide effect). This leaked optical radiation can be effectively absorbed by the semiconductor material (silicon) of a photodiode array within the area close to the illuminated pixel, creating additional crosstalk of up to 5% or more.

The crosstalk impacts were analyzed experimentally and theoretically in a number of works (see for example ref. [1-5]). Most of the published works discussed the crosstalk impact on

the image resolution and artifacts formation. It was shown that the uniform crosstalk influences mainly the image resolution, while a non-uniform crosstalk, which may be important at the boundaries of the photodetector array, results in image artifacts. The image artifacts could be either visible or not visible dependently on the amplitude of the quantum noise caused by x-ray and optical quanta (see e.g. ref. [4]). However, one important feature of the crosstalk was missed: the crosstalk itself is an additional source of the quantum noise of the pixels. In many cases this additional component of quantum noise may exceed the magnitude of all other noise sources, which may significantly decrease the signal-to-noise ratio and deteriorate the image quality. This effect was analyzed for the first time in our recent works on electrical crosstalk impact on the array pixels noise properties and detectivity [6,7]. The current paper makes emphasis on a similar analysis of the optical crosstalk impact on the photodiode arrays performance. We compare optical and electrical crosstalks measured with the back-illuminated photodiode arrays manufactured using the SEMICOA proprietary design [8-11] with the results obtained using conventional back-illuminated and front illuminated arrays.

## II. EXPERIMENTAL SETUP, SAMPLES AND METHODS

We analyzed the crosstalk impact on 2D back-illuminated, *pin* photodiode arrays with 16x16 elements. The arrays' pixel pitch was close to in both directions of 2D structure.

The SEMICOA proprietary design arrays with isolating diffusion walls between pixels (Figure 1a) as well as conventional back-illuminated arrays (without the structures isolating each pixel from its neighbors, Figure 1b) were used in the experiments and for phenomenological comparison of the crosstalk properties. The arrays thickness was 75 $\mu$ m and 100 $\mu$ m.

The gaps ("dead spaces") between adjacent elements were ~200 – 250  $\mu$ m by design. However, one should note that for the conventional back-illuminated arrays (without the isolating structures between the pixels – Figure 1b) there were no actual physical gaps between adjacent elements. The surface sensitivity of such back-illuminated photodiode arrays is usually close to its maximum across the central portion of each pixel of the array and drops close to the pixel edges. This drop of sensitivity is relatively small (usually not more than ~10-20% of the signal strength) and occurs due to the lateral transport (drift and diffusion) of non-equilibrium charges to the neighbor pixels. Such drift is considered to be the main component of the electrical crosstalk. In contrast, SEMICOA proprietary design arrays provide very good physical isolation gaps between adjacent pixels. The sensitivity of the arrays shown in Figure 1a is maximum and uniform across the pixel active area and drops by more than three orders of magnitude close to the pixel edges (within the gaps between adjacent pixels). However, non-equilibrium charges created by light absorption inside the gaps do not have chance to drift or diffuse laterally toward the neighbor pixels. Those charges recombine almost completely inside the isolation walls (gaps)

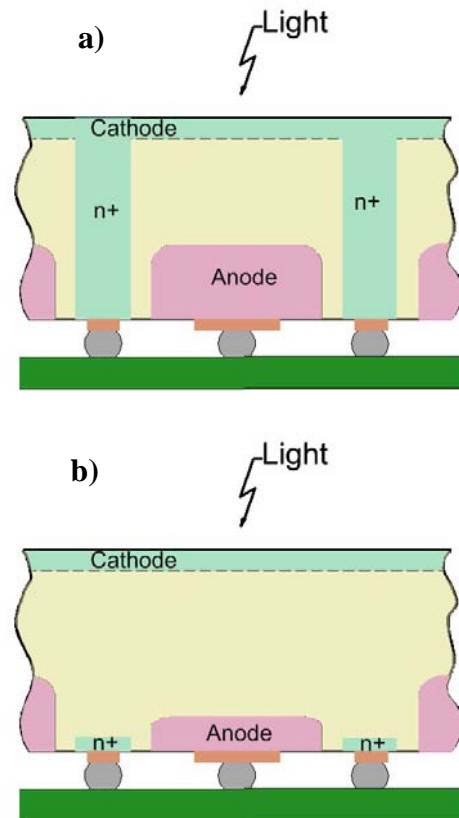


Fig.1. Schematic structure of the SEMICOA proprietary design *pin* photodiode array (a) and conventional back-illuminated *pin* photodiode array (b). The n+ isolation diffusion that propagates through the whole structure in the panel a) reduces significantly the crosstalk and improves the imaging properties of the array. See text for details.

suppressing the electrical crosstalk down to negligible values. See Figure 2 and text in the Section III below for more discussions on this topic.

For the SEMICOA proprietary design array structure (Figure 1a), each photo sensitive element can be considered as a photodiode, surrounded with isolating walls that excludes electrical crosstalk almost completely and as it will be discussed below, reduces significantly the optical crosstalk.

Arrays were flip-chip die attached to PCB that provided a possibility to connect all 256 channels of the array to the measuring system.

To measure electrical crosstalks and to estimate optical crosstalks, the arrays' monochromatic illumination was provided with either a white light source coupled to the double monochromator or light emitting diodes. Illuminating light was focused in a small diameter (10 – 40 $\mu$ m) spot on the back surface of the array. The spot size was varied dependently on the experiment requirements.

Source-measure units KEITHLEY-237 were used to record photocurrents and crosstalks from the array elements. The photodiode bias voltage was 0V in all experiments. The

measurements were made at ambient temperature  $T=23$  °C. Keithley-237 units were connected to a PC via GPIB connector interface. Labview software controlled the measurement sequence and initial data processing.

Whereas the electrical crosstalk was measured directly (the methods were described in [7, 11]), the estimation of optical crosstalks was made phenomenologically using our results for the electrical crosstalk and simple ray optics calculations for the model detector system.

### III. RESULTS

#### A. Electrical Crosstalk

The detailed analysis and description of experiments on the dc and ac electrical crosstalk measurements were presented

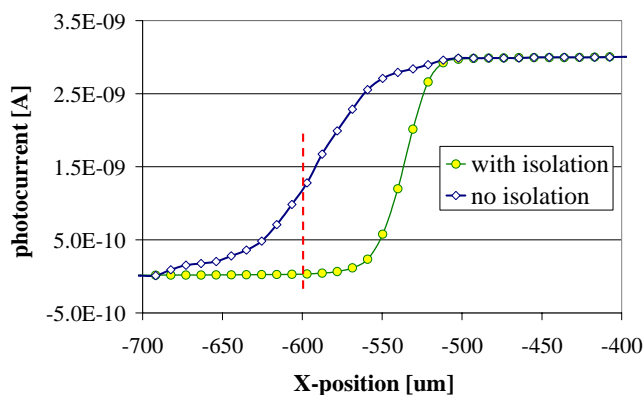


Fig. 2. Electrical crosstalk measured with the small diameter light spot scanned across the boundary between two pixels. Green line corresponds to the array with isolating diffusion walls between photodiode pixels; Blue line corresponds to the conventional design array with no isolating structure between the pixels.

elsewhere [7, 11]. Here we will briefly repeat some of the important results. Figure 2 shows typical photocurrents from photodiode pixels measured while scanning the 10-um diameter light spot ( $\lambda = 550$  nm) across the photodiode array in  $x$  direction with 10-um step size. 75um array thickness was used in this experiment.

The spot of light was scanned from the middle of one pixel to the middle of the adjacent pixel across the boundary (gap) separating the pixels (the position of the boundary between the two pixels is shown with the red dashed line). The current was recorded from one pixel whereas the anodes and cathodes of all other neighbor photodiode pixels were shorted.

The pixel photocurrent measured for the array with isolating diffusion walls between neighbors showed a well pronounced signal drop towards the gap – see green line in Figure 2. In contrast, the photocurrent for the array with no isolating diffusion dropped markedly slower towards the gap and was still well pronounced ( $>1\%$  of the maximum signal strength) even after the light spot crossed the boundary between the pixels. The smooth signal drop when approaching the pixel boundary from the right in Figure 2 was attributed to the loss of the photocurrent due to the crosstalk traversing from the illuminated (right) cell to the neighbor cell on the left.

Similarly, a non-zero photocurrent measured when light was focused to the left of the pixel boundary (red line in Figure 2) was attributed to the crosstalk flowing from the left cell to the right one.

#### B. Optical Crosstalk Due to Scattering of X-rays

This source of the crosstalk does not depend on the pin photodiode array structure; therefore, no advantage is expected for the photodiode arrays with isolation diffusion between pixels.

#### C. Optical Crosstalk Due to Penetration of Optical Quanta Through Septa

Optical photons created by deposited in a scintillator pixel x-ray quanta have a finite probability to penetrate into septa through the reflective wall separating two scintillator pixels – see the trace shown with green line in Figure 3 for the case of pin photodiode array with isolating diffusion structures between the pixels. After multiple reflections inside septa the photons escape into optical cement and penetrate the silicon crystal in the area between two photodiode pixels – see the case 3 in Figure 3. The non-equilibrium (majority) carriers generated here are effectively recombined and have only a little probability to be captured by the adjacent anode to create a crosstalk. Simplified quantitative estimations based on ray optics and experimental data on scanning the surface of the photodiode array with a small diameter light spot show that

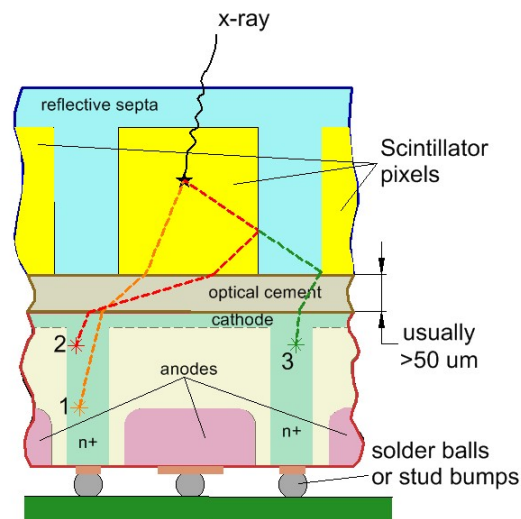


Fig. 3. Schematic block diagram of the back-illuminated, *pin* photodiode array with isolating diffusion structures and pixilated scintillator array attached on the top using optical cement. X-ray deposited in the scintillator pixel creates optical quanta, which exit the scintillator crystal and may propagate along the layer of optical cement due to a waveguide effect (red and coral lines). A portion of optical quanta penetrate through the reflective septa separating the scintillator pixels and reach the gap area between the photodiode pixels (green line). See text for more details.

over 90% of the optical crosstalk from this source can be suppressed due to charge recombination within the septa. The above estimations were made for the pixels pitch 1 mm, gaps

size 200um, and optical cement thickness 50um. The crosstalk suppression efficiency depends strongly on the overall system configuration, including alignment quality between the photodiode and scintillator arrays.

Consideration of a similar case for the back-illuminated photodiode array with no isolating structures showed that non-equilibrium charges generated by light in silicon crystal underneath the septa can be captured by the adjacent anode with high probability, creating the noticeable crosstalk – see Figure 4, case 3 (green trace).

### C. Optical Crosstalk Due to Leaking of Optical Photons Through Optical Cement

After multiple reflections inside the scintillator crystal, optical photons may enter a layer of optical cement and propagate along this layer towards the pixel's boundary. Eventually, the photons may enter silicon crystal as it is shown with the rays #1 and #2 in Figures 3 and 4.

For the case of a conventional structure, the absorbed photons create non-equilibrium charges that drift/diffuse toward the adjacent anode producing the crosstalk. See ray 1 (coral line) and ray 2 (red line) in Figure 4.

In contrast, for the case of structures with isolating diffusion between the photodiode pixels the non-equilibrium charges recombine within the area between the photodiode pixels and

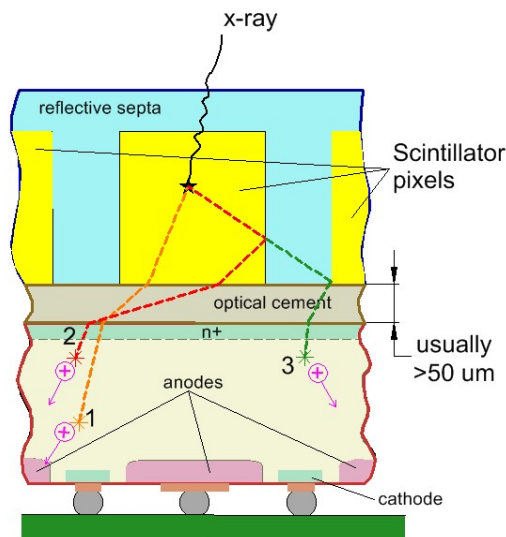


Fig. 4. Schematic block diagram of the conventional back-illuminated, *pin* photodiode array with no isolating diffusion structures and with scintillator array attached on the top using optical cement. X-ray deposited in the scintillator pixel creates optical quanta, which exit the scintillator crystal and may propagate along the layer of optical cement due to a waveguide effect (red and coral lines). A portion of optical quanta penetrate through the reflective walls separating the scintillator pixels and reach the gap area between the photodiode pixels (green line). Upon absorption by silicon crystal, optical quanta create non-equilibrium carriers that can be effectively captured by the adjacent to the irradiated cell photodiode pixel, creating crosstalk.

no additional crosstalk is produced (see red and coral lines in Figure 3). Simplified estimations for the detector structure with the pixels pitch 1 mm, gaps size 200um, and optical

cement thickness 50um showed that at least 50% of the of the crosstalk from the source discussed in this section was suppressed.

## IV. DISCUSSION

Summarizing our analysis of the crosstalk originating from four different sources, we conclude that for the photodiode array structures with isolating diffusion between pixels the total optical crosstalk can be suppressed by approximately one order of magnitude. The suppression efficiency depends on the features of the structure (pixels size, gaps size, optical cement thickness, etc.) and alignment of the photodiode array with the scintillator array. The electrical crosstalk is negligible at all for the photodiode arrays with isolating diffusion.

Crosstalk (both optical and electrical) is highly undesirable since it not only reduces the image resolution and creates image artifacts, but also decreases the detectivity of the array elements. A brief analysis below gives an estimate of the detectivity for the arrays with and without the isolating diffusion between the photodiode pixels.

Dark noise current  $i_n$  can be calculated as a sum of the thermal noise current of the photodiode dynamic resistance  $R_d$  and shot (quantum) noise current from the equation:

$$i_n^{dark} = \sqrt{2qI_{dark}\Delta f + \frac{4kT\Delta f}{R_d}}, \quad (1)$$

in which  $q$  is the elementary charge,  $\Delta f$  is the frequency bandwidth,  $k$  is the Boltzmann constant, and  $T$  is the absolute temperature. Below we consider influence of electrical and optical crosstalk on the pixel's noise current.

### A. Electrical Crosstalk Impact

Electrical crosstalk arising due to the unwanted carriers flow from the illuminated cell of the array to the adjacent cells adds an additional background current flow  $I_b$ , which increases the noise current:

$$i_n^{el} = \sqrt{2q(I_{dark} + I_b)\Delta f + \frac{4kT\Delta f}{R_d}}. \quad (2)$$

Consider experimental conditions of a typical computed tomography system, in which the x-ray flux may vary from ~5 to ~30000  $\gamma$ -photons per ~300  $\mu s$  integration time with the conversion efficiency of ~5000 optical photons per single  $\gamma$ -photon [12]. To simplify analysis, consider an ideal situation, in which the test pixel is kept in dark and radiation is deposited in the adjacent pixels only. Figure 5 shows several representative curves calculated using equation 2, experimentally measured dark leakage currents for two types of back-illuminated photodiode arrays, and electrical crosstalk measurement results discussed above in the Section III-A.

Blue line in Figure 5 shows a typical noise current of ~1.3E-15 A/ $\sqrt{Hz}$  at 10 mV reverse bias for the not illuminated cells of the array. Note that the dark noise current was practically the same low for both arrays, with and without isolating diffusion between photodiode pixels.

If the test pixel of the array with isolating diffusion was still kept in the dark and adjacent cells were illuminated, the noise current of the not illuminated pixel increased very little due to a negligibly small electrical crosstalk. Even at a very high radiation level of ~300000  $\gamma$ -photons per ~300  $\mu s$  integration

time the maximum noise current value was  $\sim 1.8\text{E-}15 \text{ A}/\sqrt{\text{Hz}}$  for  $\lambda=540 \text{ nm}$  (see the green line in Figure 5).

For the conventional back-illuminated array with a crosstalk value of  $\sim 1\%$  at  $540 \text{ nm}$  the noise current of the not illuminated (test) pixel increased significantly with illumination of the adjacent cells. See the curves in magenta, red, and brown in Figure 5 for optical fluxes of 1000, 10000, and 300000  $\gamma$ -photons per  $\sim 300 \mu\text{s}$  integration time, respectively.

### B. Optical Crosstalk and Total Crosstalk Impact

Optical crosstalk impact on noise characteristics of photodiode arrays can be treated in a similar way as electrical crosstalk, i.e. using a formalism based on the background current influence of the noise. In this case, the background current  $I'_b$  due to the optical crosstalk creates an additional component of the noise current:

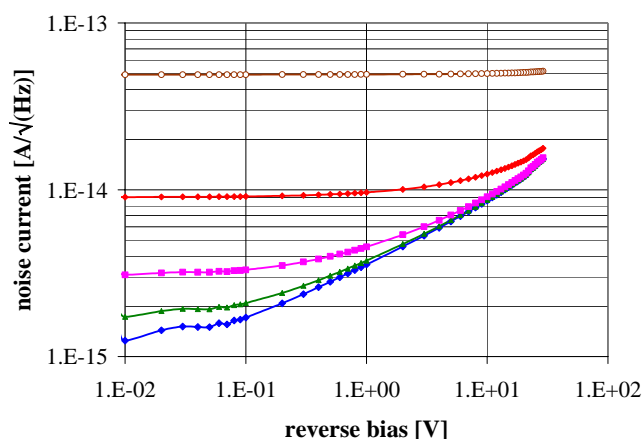


Fig. 5. Noise current for the back-illuminated array with isolating diffusion in the dark (blue line) and with the crosstalk interference at the maximum optical flux intensity level of  $\sim 5\text{E}+12 \text{ s}^{-1}$  deposited on the adjacent element (green line). Magenta, red, and brown lines show the noise currents for the conventional back-illuminated array with the crosstalk value of 1% and for the optical fluxes deposited on the adjacent cell of  $1.5\text{E}+10 \text{ s}^{-1}$ ,  $1.5\text{E}+11 \text{ s}^{-1}$ , and  $5\text{E}+12 \text{ s}^{-1}$ , respectively.  $T=25 \text{ }^\circ\text{C}$ .

$$i_n^{opt} = \sqrt{2q(I_{dark} + I'_b)\Delta f + \frac{4kT\Delta f}{R_d}} \cdot \quad (3)$$

Let us first take into account only two sources of optical crosstalk – the crosstalk originating due to optical photons penetration through the walls of the reflective septa (green lines in Figures 3 and 4) and the crosstalk arising due to wave-guiding of optical photons via a layer of optical cement (red and coral lines in Figures 3 and 4). In accordance with our estimations of Section III and in a good agreement with the results of other works [2-4], a reasonable estimate for the total optical crosstalk due to above two reasons is 5% for the conventional, back-illuminated photodiode array. For the photodiode array with isolating diffusion the optical crosstalk value is approximately 10-times smaller, i.e. 0.5%.

Figure 6 shows calculated optical crosstalk for two different arrays. The noise current due to optical crosstalk was estimated to be 3-4 times smaller for the array with isolating diffusion than that for the conventional array.

As soon as the third component of optical crosstalk – the one that originates due to x-ray scattering within the scintillator crystal does not depend on the photodiode array structure, this component produces just a parallel shift up of the green and brown curves in Figure 6.

As it is obvious from Figures 5 and 6, the noise current due to the total (electrical + optical) crosstalk,  $i_n = i_n^{el} + i_n^{opt}$ , is markedly smaller for the array with isolating diffusion than for the conventional back-illuminated photodiode array.

The advantage of a small crosstalk performance is obvious from Figure 7, in which the specific detectivity  $D^* = \frac{\sqrt{A_{det}\Delta f}}{NEP}$  versus wavelength is plotted for two different arrays using the total crosstalk estimations presented above ( $A_{det}$  is the pixel active area size and NEP is the noise equivalent power calculated as the ratio of the noise current over the spectral

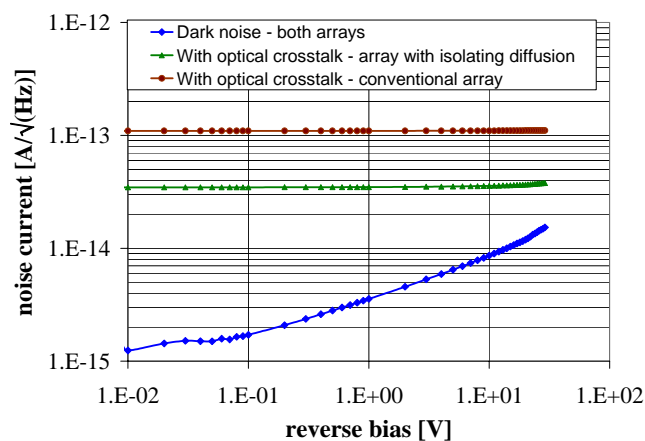


Fig. 6. Noise current for the back-illuminated arrays in the dark (blue line) and with the optical crosstalk interference at the maximum optical flux intensity level of  $\sim 5\text{E}+12 \text{ s}^{-1}$  deposited on the adjacent element (green and brown lines). Green line is the noise current for the array with isolating diffusion. Brown line shows the noise current for the conventional back-illuminated array.  $T=25 \text{ }^\circ\text{C}$ . See text for more details.

responsivity). The detectivity of conventional array drops significantly faster than that of the array with isolating diffusion due to the higher total crosstalk interference. Since the process of non-equilibrium carriers' generation via light absorption is essentially a stochastic process, the higher detectivity value for the pixels of back-illuminated array with isolating diffusion means that the same image quality may be obtained with either the smaller integration time or lower radiation flux than those for the conventional back-illuminated arrays [13]. Hence, the arrays with low electrical and optical crosstalk may provide the way for reducing the total exposure time and radiation dose in e.g. medical imaging applications.

The effect of the increased detector noise due to the crosstalk interference is rather specific since it influences mainly the immediate neighbors of the illuminated pixels and may be significant for the high contrast patterns only. However, this effect may be particularly important for the imaging systems with a relatively large pixel size, high pixels density, and small gaps between adjacent pixels.

Thin, back-illuminated photodiode arrays with isolating

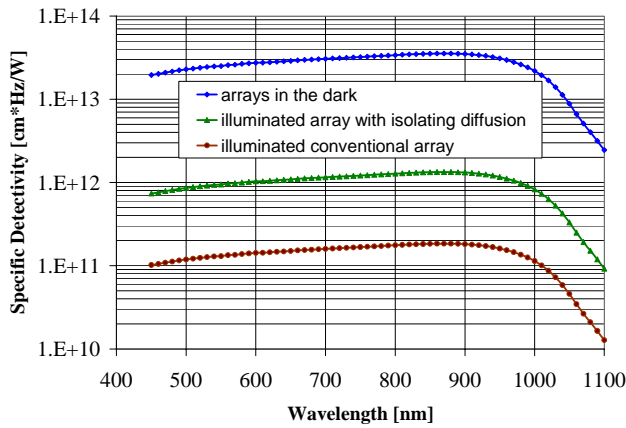


Fig.7. Specific detectivity for the back-illuminated arrays at 25 °C in the dark (blue line) and with the total crosstalk interference at the maximum optical flux intensity level for the adjacent element of  $\sim 5E+12 \text{ s}^{-1}$  (green and brown lines). Green line corresponds to the back-illuminated photodiode array with isolating diffusion. Brown line corresponds to the conventional back-illuminated array.

diffusion between pixels are close to their front-illuminated counterparts with respect to the crosstalk behavior. Due to isolating structures applied usually between the pixels of front-illuminated photodiode arrays, these arrays suppress efficiently electrical and optical crosstalk, providing usually clearer images with not as many artifacts as the conventional back-illuminated arrays. The SEMICOA proprietary design arrays present a very efficient alternative that on one side combines the advantages of the front- and back-illuminated structures and on the other side eliminates the drawbacks of the conventional designs.

#### ACKNOWLEDGEMENT

The authors acknowledge G. Papadopoulos, E. Bartley and R. Villanueva for samples preparation and A. Popp and M. Kalatsky for valuable discussions.

#### REFERENCES

[1] Utrup, S.; Chappo, M.; Harwood, B.; Krecic T.; Luhta, R.; Mattson, R.; Salk, D. and Vrettos, C. "Design and Performance of a 32 Slice CT Detector System using Back Illuminated Photodiodes". In: Medical

Imaging 2004: Physics of Medical Imaging, *Proceedings of SPIE*, Vol. 5368 (SPIE Bellingham, WA, 2004), pp. 40-51.

- [2] Ikhlef, A. and Thirvikraman, S. "Crosstalk modeling of a CT detector". In: Medical Imaging 2004: Physics of Medical Imaging, *Proceedings of SPIE*, Vol. 5368 (SPIE Bellingham, WA, 2004), pp. 906-913.
- [3] Luhta, R.; Mattson, R.; Taneja, N. and Bui, P. "Back Illuminated Photodiodes for Multislice CT: An Estimation of Temporal and Spatial Properties by Carrier Diffusion Modeling". In: Medical Imaging 2004: Physics of Medical Imaging, *Proceedings of SPIE*, Vol. 5368 (SPIE Bellingham, WA, 2004), pp. 552-563.
- [4] Engel, K.J.; Spies, L.; Vogtmeier, G. and Luhta, R. "Impact of CT detector pixel-to-pixel crosstalk on image quality". In: Medical Imaging 2006: Physics of Medical Imaging, *Proceedings of SPIE*, Vol. 6142, 61422F, (2006) · 1605-7422/06/\$15 · doi: 10.1117/12.654499.
- [5] Riviere, P.J. "Fourier crosstalk analysis of multi-slice and conebeam helical CT". In: Medical Imaging 2004: Physics of Medical Imaging, *Proceedings of SPIE*, Vol. 5368 (SPIE Bellingham, WA, 2004), 1605-7422/04/\$15 · doi: 10.1117/12.534117, pp. 19-28.
- [6] Goushcha, I., Tabbert, B., and Goushcha, A.O. "Silicon PIN Photodiode Array for Medical Imaging Applications: Structure, Optical Properties and Temperature Coefficients". In: 2005 IEEE Nuclear Science Symposium Conference Record, 0-7803-9221-3/05/\$20.00 ©2005 IEEE, p. 2840-2843.
- [7] Goushcha, I., Tabbert, B., and Goushcha, A.O. "Noise performance and temperature coefficients studies for the back-illuminated, thin silicon pin photodiode arrays". In Semiconductor Photodetectors III, edited by Marshall J. Cohen, Eustace L. Dereniak, Proc. of SPIE Vol. 6119, 61190C, (2006) · 0277-786X/06/\$15 · doi: 10.1117/12.644958.
- [8] Goushcha et al., United States Patent No. 6,672,473 B1, Jul 13, 2004.
- [9] Goushcha et al., United States Patent No. 7,112,465 B2, Sep. 26, 2006.
- [10] Tabbert, B., Hicks, C., Bartley, E., Wu, H., Goushcha, I., Metzler, R.A., and Goushcha, A.O. "The structure and physical properties of ultra-thin, multi-element Si pin photodiode arrays for medical imaging applications". In: Medical Imaging 2005: Physics of Medical Imaging, *Proceedings of SPIE*, Vol. 5745 (SPIE Bellingham, WA, 2005), pp. 1146-1154.
- [11] Goushcha, I., Tabbert, B., and Goushcha, A.O. Silicon PIN Photodiode Array for Medical Imaging Applications: Structure, Optical Properties and Temperature Coefficients. In 2005 IEEE Nuclear Science Symposium Conference Record, J03-12, 2840-2843.
- [12] R. Steadman, R.; Serrano, F.M.; Vogtmeier, G.; Kemna, A.; Oezkan, E.; Brockherde, W. and Hosticka, B.J. "A CMOS photodiode array with in-pixel data acquisition system for computed tomography". *IEEE J. Solid State Circuits*, Vol. 39, pp. 1034-1043, 2004.
- [13] M.F. Kijewski and P.F. Judy, The noise power spectrum of CT images, *Phys. Med. Biol.*, Vol. 32, pp. 565-575, 1987.